The Plant Cell, Vol. 17, 375–388, February 2005, www.plantcell.org © 2005 American Society of Plant Biologists

Mx-rMx, a Family of Interacting Transposons in the Growing *hAT* Superfamily of Maize [W]

Zhennan Xu[a,b] and Hugo K. Dooner[a,b,1]

[a] Waksman Institute, Rutgers University, Piscataway, New Jersey 08855
[b] Department of Plant Biology, Rutgers University, New Brunswick, New Jersey 08901

More than half a century after the discovery of transposable elements, the number of genetically defined autonomous elements that have been isolated and characterized molecularly in any one species remains surprisingly small. Because of its rich genetic history, maize (*Zea mays*) is, by far, the plant with the largest number of such elements. Yet, even in maize, a maximum of only two autonomous elements have been characterized in any transposon superfamily. This article describes the isolation and molecular and genetic characterization of *Mx* (for mobile element induced by x-rays), a third autonomous member of the *hAT* transposon superfamily in maize. *Mx* is 3731 bp long, ends in 13-bp terminal inverted repeats (TIRs), and causes an 8-bp duplication of the target site. *Mx* and *rMx* (for responder to *Mx*), its 571-bp nonautonomous partner, define a classical family of interacting transposable elements. Surprisingly, the TIRs of *Mx* and *rMx* are only 73% identical, and the subterminal sequences are even less so, suggesting that *Mx* and *rMx* may represent diverging transposable elements still capable of mobilization by the same transposase. Sequences that are closer to the ends of either *Mx* or *rMx* are present in the maize genome. *Mx* is predicted to encode a 674–amino acid protein that is homologous to the *Ac* transposase. Although *Mx* and *Ac* are closely related, they do not interact. Other data suggest that maize may possess at least five families of *hAT* transposons that do not interact with each other. The possible origin of noninteracting transposon families within the same superfamily is discussed.

INTRODUCTION

Interrelationships between transposable elements in maize (*Zea mays*) have been established traditionally by complementation tests between a nonautonomous element residing at a reporter allele and an autonomous element residing elsewhere. If the elements complement to produce a mutable or unstable reporter phenotype, they are considered to belong to the same system (McClintock, 1956b) or family (Fedoroff, 1983). If they do not, they are assigned to different families. The application of this deceptively simple, yet effective, test has led to the grouping of transposons causing a wide range of mutable phenotypes in maize into several families (Peterson, 1988), of which the best characterized are *Ac-Ds*, *Spm/En-dSpm/I*, and *MuDR-Mu1*.

The subsequent DNA sequence analysis of genetically active transposons has permitted their independent classification into larger groups, termed superfamilies, based generally on three criteria: the sequence of the transposon terminal inverted repeats (TIRs), the homology of their putative transposases, and the size of the host target site duplication (TSD). The five main superfamilies of DNA transposons recognized in plants are *hAT*, CACTA, *Mutator*, *PIF/Harbinger*, and *Tc1/mariner*, each defined by one or more genetically characterized founding members (Feschotte et al., 2002a). The numerous transposon-related sequences uncovered by the genome sequencing projects in Arabidopsis (*Arabidopsis thaliana*; Arabidopsis Genome Initiative, 2000) and rice (*Oryza sativa*; Goff et al., 2002) have been placed into one or another of these five large categories. Although the biological activity of these sequences has not been examined, most are expected to be immobile. In fact, miniature inverted-repeat transposable elements—the predominant transposons in or near genes—are so stable that they have been exploited as genetic markers in both maize and rice (Feschotte et al., 2002b).

The situation in maize differs from that in Arabidopsis and rice in that many genetically defined transposable element families were identified decades before the establishment of a genome sequencing project. The maize inbred lines B73 and Mo17 that have been chosen for sequencing by the public (Cone et al., 2002) and private (Palaisa et al., 2003) sectors, respectively, are not likely to carry active transposable elements, as they are known to lack even the more common ones, such as *Uq* (Cormack et al., 1988). However, active transposons are certainly present in wild populations and even in some inbred lines (e.g., van der Walt and Brink, 1969; Montanelli et al., 1984; Peterson and Salamini, 1986; Cormack et al., 1988). The extreme natural diversity in maize and its long history as a model organism for genetic research have contributed to the identification, genetic characterization, and preservation of many systems of mutability (Peterson, 1988; Neuffer et al., 1997; http://w3.ag.uiuc.edu/maize-coop/mgc-info.html), only a fraction of which have been characterized molecularly. For example, the autonomous transposons *Dt* (Rhoades, 1938), *Fcu* (Gonella and Peterson,

[1] To whom correspondence should be addressed. E-mail dooner@waksman.rutgers.edu; fax 732-445-5735.
The author responsible for distribution of materials integral to the findings presented in this article in accordance with the policy described in the Instructions for Authors (www.plantcell.org) is: Hugo K. Dooner (dooner@waksman.rutgers.edu).
[W] Online version contains Web-only data.
Article, publication date, and citation information can be found at www.plantcell.org/cgi/doi/10.1105/tpc.104.027797.

1977), *Mrh*, and *Mut* (Rhoades and Dempsey, 1982) have yet to be isolated. In some instances, a nonautonomous element of the family has been isolated and sequenced, allowing its tentative assignment to a superfamily based on TIR homology and TSD size. By those criteria, *rDt* (Brown et al., 1989) and *rMut* (Dennis et al., 1988) would be members of the *hAT* superfamily, and *rMrh* (Shepherd et al., 1989) would be a member of the *Mutator* superfamily. Further molecular characterization of these families awaits the isolation of their respective autonomous transposons.

In spite of the paucity of autonomous transposons isolated in plants (Feschotte et al., 2002b; Kunze and Weil, 2002), it is clear that several distinct transposon families belonging to the same superfamily can coexist in one species. Thus, in maize, the *hAT* superfamily includes *Ac-Ds* and *Bg-rBg* (Hartings et al., 1991b); the CACTA superfamily includes *Spm/En-dSpm/I* and *Shooter* (Panavas et al., 1999), and the *Mutator* superfamily includes *MuDR* (Walbot and Rudenko, 2002) and *Jittery* (Xu et al., 2004). This means that each superfamily contains groups of related transposons that do not interact with each other, raising the issue of how related autonomous transposons in the same species can evolve different specificities.

This article describes the isolation and characterization of *Mx* (for mobile element induced by x-rays), a new autonomous transposon of the *hAT* superfamily in maize. This transposon is responsible for the instability of *bz-x3m*, a mutation from an X-irradiated stock (Mottinger, 1973) that carries a nonautonomous element termed *rMx* (for responder to *Mx*) (Mottinger, 1992). *Mx* is more closely related to *Ac* and the *Tam3* element of *Antirrhinum majus* (Hehl et al., 1991) than to *Bg* or the *Tag1* element of Arabidopsis (Liu and Crawford, 1998), but cannot *trans*-activate *Ds* excision nor contribute to *Ac*'s dosage effect. Surprisingly, the TIRs of *Mx* and *rMx* are only 73% identical, and the subterminal sequences are even more different, suggesting that *Mx* and *rMx* may represent diverging transposable elements that can still interact with each other. The possible origin of noninteracting transposon families within the same superfamily is discussed.

RESULTS

Isolation and Characterization of *rMx*, the Nonautonomous Element of the *Mx-rMx* System

The *bz-x3m* mutation was acquired from John Mottinger in 1982 and introduced into the genetic background of the W22 inbred by backcrossing repeatedly to a W22 *sh bz-R wx* tester line and selecting bz-m spotted seed each generation. After the fourth backcross, a *Sh bz-x3m wx* stock was established by self-pollinating the heterozygous BC4 plants and identifying progeny plants that produced mostly spotted seed and did not segregate *sh* in their selfed ears. These plants were the foundation of the W22 *bz-x3m* stock used in the work described below. The W22 *bz-x3m* stock produces a finely spotted kernel phenotype (Figures 1A and 1B), similar to that described earlier by Mottinger (1973) (1992), except that the frequency of somatic reversion appears to be lower in the W22 version. Both stocks behave similarly, though, in that the overall somatic reversion level (kernel spot size and number) is higher when they are used as female, rather than male, parents in crosses to a *bz-R* tester. As in the original mutant, some kernels are uniformly bronze and lack obvious *Bz′* revertant sectors, but most do not breed true. In the presence of the *R-r* transcription factor carried by most color-converted W22 lines (Brink, 1956), the somatic instability of *bz-x3m* is also evident as red sectors in otherwise bronze anthers (Figure 1C).

Figure 1. *bz-x3m* Phenotypes.

(A) Ear of a W22 *bz-x3m* homozygote, showing the finely spotted kernel phenotype arising from late somatic reversions in the aleurone layer. A few kernels show larger sectors produced from earlier reversion events.
(B) Close-up of **(A)**, showing the small size of the majority of revertant sectors in the aleurone.
(C) Spotted and red anthers in a W22 *bz-x3m* homozygote. Most reversions occur late in development and result in very finely spotted anthers. However, reversions can also occur earlier, as indicated by the two florets with exclusively red anthers.

Mottinger (1992) established that the mutability of *bz-x3m* was because of an ~0.5-kb nonautonomous element at *bz*, which he designated *rMx*, and a closely linked autonomous element, which he designated *Mx*. To characterize this transposable element system more fully, the *rMx* insertion in *bz* was PCR amplified with *bz* primers and sequenced. *rMx* is 571 bp long, has 13-bp imperfect TIR, contains 15 copies of the hexanucleotide CCCGAA or its reverse complement within the subterminal 170 bp at either end, and produces an 8-bp TSD. The *rMx* insertion site (GTGGAGGA) is located in the *bz* second exon, close to the 3′ end of the gene. The sequences of the 13-bp imperfect TIRs are 5′-TAGCACTGGGCAT-3′ at the 5′ end and 5′-ATGCCCAGTCCTA-3′ at the 3′ end (the imperfect noncomplementary bases are underlined). Sequences homologous to *rMx* are present in ~15 copies in a W22 background (data not shown).

BLASTX analysis of the GenBank sequence databases using the *rMx* sequence as query established that *rMx* had no significant similarity to any known protein. By contrast, BLASTN analysis revealed that the terminal 180 bp at either end of *rMx* were highly similar to the ends of the *Tz86* transposon. *Tz86* is a maize endogenous transposon identified in a *sh1* mutable allele

recovered after virus infection (Mottinger et al., 1984). Although *Tz86* has not been sequenced, 250 bp of each *Tz86-sh1* junction are available from GenBank (M10174 and M10175). Figure 2 shows the sequence alignment of the *Tz86* and *rMx* ends. *Tz86* and r*Mx* are 77% identical from position 1 to 181 at the 5′ end (140/181) and 81% identical from position 402 to 571 at the 3′ end (137/170). The high identity of their ends suggests that *rMx* and *Tz86* may belong to the same transposon superfamily. However, the internal part of *rMx* (from position 182 to 401) shows little similarity to the rest of the *Tz86* sequence.

bz-x3m is a mutable allele that reverts occasionally to *Bz′* (full purple) in the germ line (Mottinger, 1992). In testcrosses using the W22 *bz-x3m* stock as female parent, the frequency of *Bz′* germinal revertants is ~0.5%. To investigate whether *rMx* produces typical transposon footprints upon excision, the transposon empty sites of eight independent *Bz′* revertants were PCR amplified and sequenced. The results are presented in Table 1. The *Bz′* germinal revertants had footprints of 8+0, 8+3, 8+6, and 8+9 (i.e., nucleotide additions in multiples of three), in agreement with the requirement for restoration of the correct reading frame in *Bz′* functional derivatives. Mutations of *bz-x3m* to a stable bronze form are harder to identify because of the incomplete penetrance of the *bz-x3m* mutation, even in self-pollinated ears (Mottinger, 1992). However, one such derivative was evident as a large premeiotic sector of plump, bronze seeds in the testcross ear of a *Sh bz-x3m/sh bz-R* heterozygote. In this nonfunctional *bz-s* derivative, *rMx* had not excised, but had, instead, caused

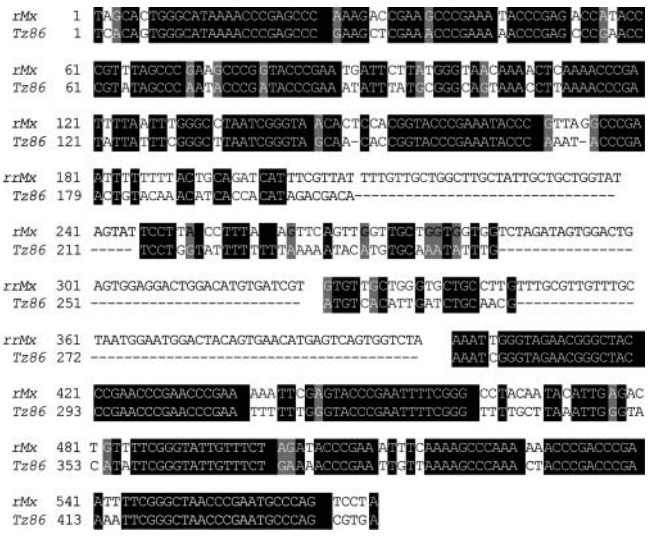

Figure 2. DNA Sequence Comparison between *rMx* and *Tz86*.

The entire 571-bp *rMx* element from *bz-x3m* was compared with the *Tz86* ends. The *Tz86* sequence is a 439-nucleotide composite, consisting of 207 nucleotides from the 5′ end (GenBank accession M10174) and 232 nucleotides from the 3′ end (GenBank accession M10175). Sequences were aligned using the program MultiAlin (http://prodes.toulouse.inra.fr/multalin/multalin.html). The graphical output highlights identical nucleotides as white letters in black boxes and purine transitions as white letters in gray boxes (Box-Shader 3.21, http://www.ch.embnet.org/software/BOX_form.html).

Table 1. *rMx* Germinal Excision Footprints in *bz-x3m*

Selections	Sequence of Empty Site			Excision Pattern
bz-x3m	GTGGAGGA	***rMx***	GTGGAGGA	
Bz′-1	GTGGAGGA			8+0
Bz′-2	GTGGAGGA			8+0
Bz′-3	GTGGA	c	GAGGA	8+3
Bz′-4	GTGGAG	c	TGGAGGA	8+6
Bz′-5	GTGGAG	c	TGGAGGA	8+6
Bz′-6	GTGGAG	c	TGGAGGA	8+6
Bz′-7	GTGGAGG	tcc	TGGAGGA	8+9
Bz′-8	GTGGAGG	tcc	TGGAGGA	8+9
bz-s1	214 bp deletion	***rMx***	GTGGAGGA	Adjacent deletion

a deletion of 214 bp of *bz* sequences immediately proximal to the insertion (Table 1). Such adjacent deletions are also generated by other plant transposable elements, such as *Mu1* (Taylor and Walbot, 1985) and *Ac* (Dooner, 1985), and probably arise from abortive excision events.

Separation and Resynthesis of *Mx* and *rMx*

To isolate and characterize the autonomous *Mx* element molecularly, it is first necessary to derive stocks in which *Mx* and *bz-x3m* have been separated so that *Mx* can be scored genetically on the basis of its ability to *trans*-activate the excision of *rMx* from *bz-x3m*. Mottinger (1992) was able to separate the nonautonomous *bz-x3m* mutant from *Mx* and, thus, to map the location of the autonomous element in his stocks. Not surprisingly for a mobile element, *Mx* did not map to a single locus in the maize genome. In addition to a location tightly linked to *bz*, *Mx* could occupy other locations: one was distal to *c1* on the same chromosome and another one was unlinked to *bz*. The genetic tests described below show that, in the W22 *bz-x3m* stock, *Mx* is present in a single copy that maps distal to the *sh* locus.

Figure 3 diagrams the crossing scheme used to separate *Mx* and *rMx*. For ease in presentation, *Mx* is shown on the *bz-x3m* parental chromosome at the location deduced from the experiment itself. Hence, the genotype of the W22 *bz-x3m* stock is represented as *Mx Sh bz-x3m wx*. That stock was crossed to a *sh Bz Wx* stock, and the resulting *Mx Sh bz-x3m wx*/+ *sh Bz Wx* F1 heterozygote was testcrossed to *sh bz-R wx* to select reciprocal recombinants between *sh* and *bz*. None of the *sh bz wx* crossovers (Figure 3, right) had spots and all of them bred true (putative + *sh bz-x3m wx*/+ *sh bz-R wx*), suggesting that *Mx* was located distal to *sh* on *9S*. These recombinants were confirmed by DNA gel blots to carry *rMx* in *bz* (data not shown), so they should serve as bona fide *Mx* testers. This inference was confirmed by further analysis of the reciprocal Sh Bz Wx recombinants.

The Sh Bz Wx crossovers (putative *Mx Sh Bz Wx*/+ *sh bz-R wx* at the left of Figure 3) were backcrossed to *sh bz-R wx*, and Sh bz wx second-cycle recombinants were obtained. The Sh bz wx recombinants should be *Mx Sh bz-R wx*/+ *sh bz-R wx* in genotype because *Mx* was inferred to be distal to *Sh*. The putative genotypic assignment of these recombinants was verified by crossing them to the *Mx* tester line described above

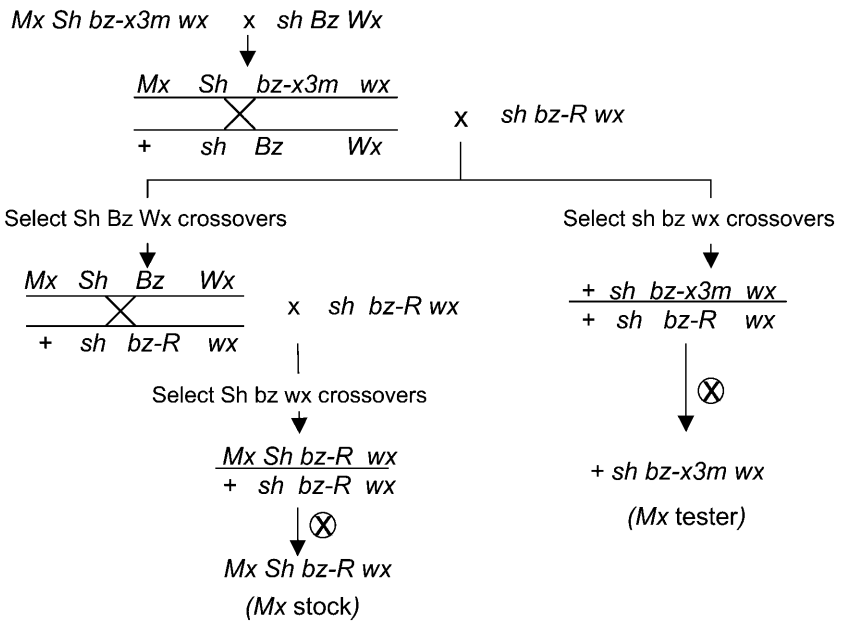

Figure 3. Genetic Scheme to Separate *Mx* and *rMx* in the W22 *bz-x3m* Stock.

See text for details.

(+ *sh bz-x3m wx*) and establishing that they could reactivate spotting (i.e., *rMx* somatic excision) in the *Mx* tester. At the same time, the W22 *sh bz-R wx* parental line was confirmed to lack *Mx* activity because it could not reactivate spotting in the *Mx* tester. Neither could several other W22 lines tested, indicating that *Mx* is not present in the W22 inbred. Although the original *bz-x3m* stock appeared to have an *Mx* element distal to *sh* and a second one between *sh* and *bz* (Mottinger, 1992), the derived W22 *bz-x3m* stock lacks the latter. Most likely, the second *Mx* element transposed and was lost during the introgression of the *Sh bz-x3m* chromosome segment into a W22 background.

Isolation and Characterization of *Mx*, the Autonomous Element of the *Mx-rMx* System

Stepwise Isolation of Progressively Larger Members of the Mx Family by Primer Walking

Hybridization of DNA gel blots with the short *rMx* probe failed to identify any bands that cosegregated with the *Mx* element in the *Mx Sh bz-R wx* and + *sh bz-x3m wx* recombinants of Figure 3. To generate a more suitable probe for the isolation of *Mx*, a three-step PCR procedure was developed based on the fact that all known autonomous maize transposons have defective relatives in the genome that have undergone internal deletions of varying lengths (Kunze and Weil, 2002; Walbot and Rudenko, 2002). The procedure, diagrammed in Figure 4A and henceforth referred to as primer walking, allowed the amplification of progressively larger members of the *Mx* family.

First, using primers from *rMx* sequences just three nucleotides away from either end (p1 and p2 in Figure 4A), a 0.8-kb band, designated *dMx1*, and the expected 0.5-kb *rMx* band were PCR amplified from total genomic DNA of the W22 *Mx bz-x3m* stock (Figure 4B) and sequenced. The ends of *dMx1* (166 bp) are highly similar (81%) to the *rMx* ends and identical to the *Tz86* ends in the database. However, the *dMx1* internal region is novel and shows no similarity to that of *rMx*. Second, using primers based on this internal region (p3 and p4 in Figure 4A), a 2.2-kb fragment, designated *dMx2*, was PCR amplified (Figure 4C) and sequenced. BLASTX analysis predicts that *dMx2* encodes an incomplete protein with homology to the *Ac* transposase. Therefore, the *dMx2* fragment is derived from a member of the *hAT* superfamily of transposons. Third, using primers based on the *dMx2* internal region (p5 and p6 in Figure 4A), a 3.0-kb fragment, designated putative *Mx*, was PCR amplified (Figure 4D) and sequenced. Consistent with the notion that this fragment comes from *Mx*, the putative *Mx* band was only amplified from the W22 *Mx bz-x3m* stock, but not from the W22 *bz-R* line. Analysis of the putative *Mx* sequence revealed that this fragment also encodes a putative *Ac*-like transposase.

Isolation of Mx

A DNA gel blot of the recombinant individuals shown in Figure 3 was then hybridized sequentially with probes made from the PCR amplification products described above. A probe from the 2.2-kb *dMx2* fragment (Figures 4A and 4C) revealed the presence of a unique *Eco*RI band in the W22 *Mx bz-x3m* parent and the *Mx Sh bz-R wx*/+ *sh bz-R wx* recombinants (Figure 5A, lanes P1 and 1 to 7), but not in the + *sh bz-x3m wx*/+ *sh bz-R wx* reciprocal recombinants or the *sh Bz Wx* and *sh bz-R wx* parents (Figure 5A, lanes 8 to 13, P2, and P3). Thus, the unique band cosegregates with *Mx* activity. Similar unique bands were also detected in gel blots of DNAs digested with either *Sal*I, *Sac*I, or *Bgl*II (data not shown).

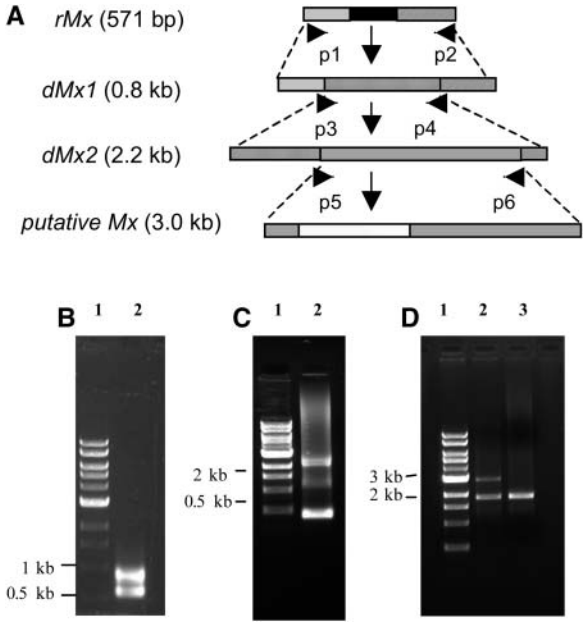

Figure 4. Primer Walking to Isolate *Mx*.

(A) Sequential PCR steps to amplify progressively larger members of the *Mx* family. p1 to p6 stand for specific primers used in the amplification reactions. Boxes with same shading indicate identical or highly similar sequences.

(B) Ethidium bromide (EtBr)–stained agarose gel of PCR amplification products with primers p1 and p2. Lane 1, 1-kb ladder of molecular size markers; lane 2, PCR products from *Mx bz-x3m*, showing the 0.8- and 0.5-kb bands, corresponding to *dMx1* and *rMx*, respectively.

(C) EtBr-stained agarose gel of PCR amplification products with primers p3 and p4. Lane 1, 1-kb ladder of molecular size markers; lane 2, PCR products from *Mx bz-x3m*, showing the 2.2-kb band corresponding to *dMx2*.

(D) EtBr-stained agarose gel of PCR amplification products with primers p5 and p6. Lane 1, 1-kb ladder of molecular size markers; lane 2, PCR products from *Mx bz-x3m*, showing the 3.0-kb band corresponding to the putative *Mx* element; lane 3, PCR products from W22 *bz-R*.

The missing ends of the putative *Mx* element (Figure 4A) and the chromosomal region flanking it (*tmx*) were amplified by inverse PCR (IPCR) using a gel-purified, *dMx2*-hybridizing, *Sal*I fragment from the *Mx bz-x3m* line as template and primers located near the ends of the putative *Mx* sequence. Rehybridization of the recombinants' DNA gel blot with the *tmx* probe (Figure 5B) supports the premise that *tmx* corresponds to the region flanking *Mx*. *tmx* detects a single polymorphic *Eco*RI band in the three parents used in the crossing scheme of Figure 3. The band present in the P1 *Mx Sh bz-x3m* parent is also present in all the *Mx Sh bz-R wx*/+ *sh bz-R wx* recombinants (lanes 1 to 7), but is absent in the + *sh bz-x3m wx*/+ *sh bz-R wx* recombinants (lanes 8 to 13). These recombinants have, instead, the band that is present in the P2 *sh Bz Wx* parent. Finally, the band present in the P3 *sh bz-R wx* testcross parent is shared, as expected, with all of the recombinants. Using *tmx* as a probe on recombinant inbred membranes (Burr et al., 1988), the putative *Mx* was mapped to a location 2 centimorgan (cM) distal to *c1* and 6 cM distal to *sh1* on *9S* (data not shown). The *tmx* polymorphism between the P2 and P3 parents can be explained by linkage drag during the derivation of those lines, which are known to carry different *c1* alleles: P2 carries a *C1-s* (super-*C1*) allele, whereas P3 carries a regular *C1* allele. The DNA gel blot data is thus consistent with the genetic crossover results shown in Figure 3.

The above hybridization data show that the putative *Mx* element, isolated by a combination of PCR primer walking and IPCR, cosegregates with *Mx* activity and resides at a chromosomal location (*tmx*) consistent with the mapped position of *Mx* in the W22 *Mx bz-x3m* stock. That this element is in fact the autonomous *Mx* transposon was confirmed by the following genetic test. Excision losses of *Mx* from the W22 *Mx bz-x3m* stock were sought in a screen for exceptional nonspotted seeds among the seed progeny of a cross to *sh bz-R wx*. Several uniformly bronze exceptions were obtained among 144 spotted seeds. Three of these exceptions bred true, producing no spotted seeds in their self-progenies. Crosses of these three exceptions to the *Mx bz-R* stock (Figure 3, left) yielded spotted seeds, indicating that the *bz-x3m* allele was intact and that somatic excision of *rMx* from *bz* could be reactivated. Crosses of the exceptions to the *Mx* tester + *sh bz-x3m* (Figure 3, right) yielded only bronze seeds, indicating that *Mx* had been lost from the genome. DNA gel blot analysis of the exceptions (Figure 6) showed they had lost the *Eco*RI band corresponding to the putative *Mx* element (arrowhead, cf. Figure 5), thus verifying the latter's identity as the true *Mx*. Using primers based on the *tmx* sequence, the *Mx* excision site in these exceptions was amplified

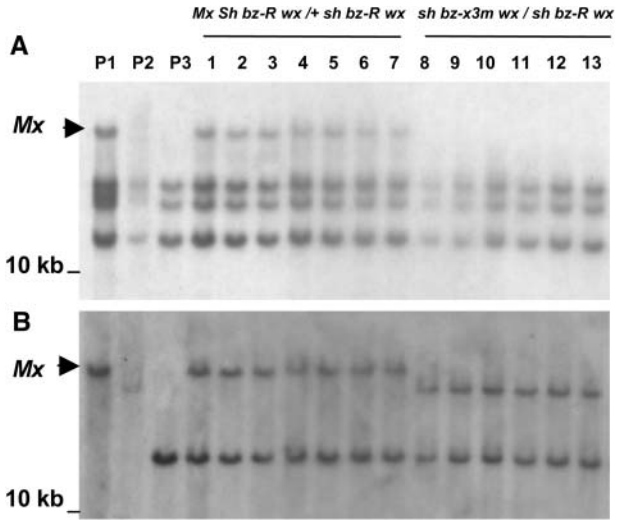

Figure 5. DNA Gel Blot Analysis of Recombinants from the W22 *Mx bz-x3m* Stock.

Reciprocal recombinants from *Mx Sh bz-x3m*/+ *sh Bz* heterozygotes were obtained by the scheme diagrammed in Figure 3. Genomic DNA was digested with *Eco*RI, blotted onto Nylon membranes, and hybridized sequentially to radiolabeled probes from *dMx2* **(A)** (Figure 4A) and *tmx* **(B)**, the *Mx* flanking region. P1, *Mx Sh bz-x3m wx* parent; P2, *sh Bz Wx* parent; P3, *sh bz-R wx* testcross parent; lanes 1 to 7, *Mx Sh bz-R wx*/+ *sh bz-R wx* recombinants; lanes 8 to 13, + *sh bz-x3m wx*/+ *sh bz-R wx* recombinants. The arrowhead identifies the position of *Mx*.

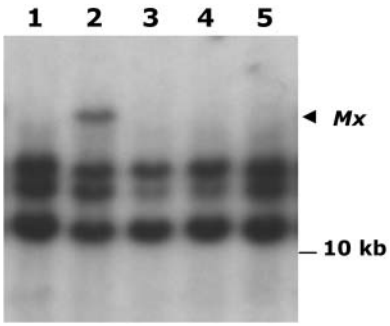

Figure 6. DNA Gel Blot Analysis of Exceptions from *Mx bz-x3m* That Have Lost *Mx*.

Genomic DNA was digested with *Eco*RI, blotted onto nylon membranes, and hybridized to a radiolabeled probe from *dMx2*. Lane 1, the *Mx* tester line + *sh bz-x3m wx*; lane 2, *Mx Sh bz-x3m*; lanes 3 to 5, three + *Sh bz-x3m* derivatives from *Mx Sh bz-x3m*. The arrowhead identifies the position of *Mx*.

and sequenced. Examination of the sequence revealed that *Mx* had excised and left typical transposon footprints at the empty site (Table 2). The demonstration that the somatic excision of *rMx* from *bz-x3m* can be activated in a stock carrying the putative *Mx* element, but not in derivatives lacking it, establishes unambiguously that that element is *Mx*.

Mx Is a Member of the *hAT* Transposon Superfamily

A complete *Mx* transposon was amplified using *tmx* primers and sequenced. Figure 7A diagrams the overall structure of the element. *Mx* is 3731 bp long, ends in 13-bp imperfect TIRs identical to those of *Tz86*, contains 17 subterminal direct repeats of the hexanucleotide CCCGAA or its reverse complement, and causes an 8-bp duplication of the target site (5′-CACTACAC-3′). The 180-bp terminal sequences at the 5′ and 3′ ends, respectively, are only 76 and 78% similar to those of *rMx*, but are identical with those of *dMx1* and *Tz86*. Thus, *Mx* and *Tz86* may be the same element, based on the limited *Tz86* sequence available. The *Mx* transcript is predicted to consist of three exons encoding a 674–amino acid protein that is homologous to the *Ac* transposase. Figure 7B shows the sequence alignment of the proteins encoded by *Mx* and *Ac*. Like the *Ac* transposase, the protein encoded by *Mx* contains three domains, designated hAT1, hAT2, and hAT3, which are highly conserved among members of the *hAT* transposon superfamily (Kunze and Weil, 2002). This large superfamily has been named after the autonomous elements *hobo* in *Drosophila melanogaster*, *Ac* in maize, and *Tam3* in Antirrhinum (Calvi et al., 1991) and includes transposons from plants, animals, and fungi.

Transposition of *Mx*

To confirm that *Mx* could reinsert in the genome, as suggested by earlier mapping data (Mottinger, 1992), the spotted seed progeny from the testcross of a *Mx Sh bz-x3m*/+ *sh bz-R* heterozygote was screened for new *Mx*-hybridizing bands by DNA gel blots. Out of 95 individuals analyzed, two had novel bands, but retained *Mx* at its original location (Figure 8, lanes 5 and 6). This outcome—the joint recovery of transposon copies at both donor and receptor sites—is also common in *Ac* transposition (Chen et al., 1987). As indicated below, the alternative outcome—loss of the transposon copy at the donor site—was also uncovered, suggesting that *Ac* and *Mx* may transpose by the same mechanism (Brink and Nilan, 1952; Greenblatt and Brink, 1962). *Mx* transposants that have lost *Mx* from its original position were found serendipitously during the reprobing with an *Mx* probe of a blot containing the DNA of a small number of spotted progeny from a cross between *Mx Sh bz-x3m* and *sh bz-R*. The pattern of *Mx*-hybridizing bands in these individuals is shown in Figure 8 (lanes 3 and 4), and the sequence of their *Mx* excision sites is given in Table 2 (xis4 and xis5). Thus, as with *Ac*, transposition of *Mx* may or may not result in a net increase in the original copy number of the transposon (Chen et al., 1987, 1992).

Mx Homologous Sequences in Maize and Its Relatives

An *rMx* probe, which shares homology with *Mx* only at its ends, detects multiple bands in W22 (data not shown). To examine the relative abundance of *Mx* homologous sequences in maize and its closest relatives, a blot containing DNA from several maize inbred lines and teosinte accessions was hybridized with an *Mx* internal sequence. The probe sequence, which extends from position 760 to 1710 and includes part of the *Mx* first exon (Figure 7A), is completely missing in the two *dMx* elements isolated in this study (Figure 4A), so it will not detect these or other similarly deleted defective *Mx* elements. Figure 9 shows the hybridization result. The 10 different Corn Belt inbreds examined are as follows: A188, A636, B73, BSSS53, 4Co63, H99, M14, Mo17, W22, and W23 (lanes 6 to 15). The five teosinte plants examined came from two different collections of *Z. mays* ssp *mexicana* (lanes 1 and 2, from Estado, Mexico, and lane 5, from Michoacán) and one collection of *Z. mays* ssp *parviglumis* (lanes 3 and 4, from Michoacán). *Mx* internal sequences are present in low copy number (one to four) in the maize inbreds and in somewhat higher copy number (five to nine) in the teosinte plants, which are known to be highly heterozygous. The potential *Mx* activity of those sequences in the inbreds in A636, B73, 4Co63, H99, M14, and Mo17 was tested by crossing each of them to an *Mx* tester line (see Figure 3) and scoring for bz-m kernels in the F2 progeny.

Table 2. Analysis of *Mx* Excision Footprints

Selections	Sequence of Empty Site			Excision Pattern
Mx-TSD	CACTACAC	***Mx***	CACTACAC	
Mx-xis1[a]	CACTACAC	gtg	CACTACAC	8+9
Mx-xis2[a]	CACTACA	g	CTACAC	8+6
Mx-xis3[a]	CACTACA	gt	ACTACAC	8+8
Mx-xis4[b]	CACTACAC			8+0
Mx-xis5[b]	CACTACA	gt	ACTACAC	8+8

[a] *Mx* excisions xis1, xis2, and xis3 were identified as nonspotted exceptions in a *Mx- bz-x3m* × *bz-R* cross.

[b] *Mx* excisions xis4 and xis5 were identified by DNA blots among the spotted individuals in the same cross.

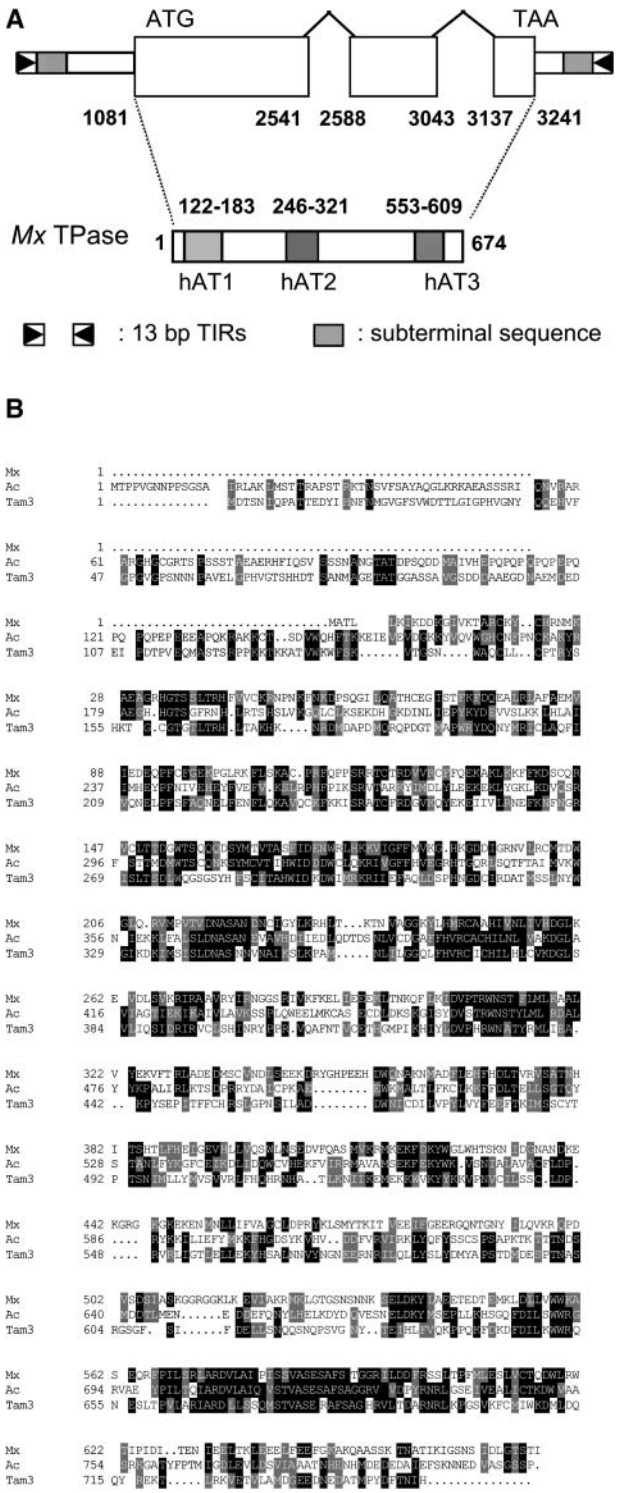

Figure 7. *Mx* Structure and Sequence Comparison.

(A) Structure of *Mx*, showing the location of the 13-bp TIRs, the subterminal hexanucleotide repeats, and the exons and introns of its predicted protein, *Mx* TPase. This protein is homologous to the transposases encoded by *Ac* and other members of the *hAT* transposon superfamily, which share three conserved domains, indicated as hAT1, hAT2, and hAT3.

Eight F2 ears were scored for each inbred and no bz-m seed were found. This test would have detected an active *Mx* element anywhere in the genome, except at locations very closely linked (<1 cM) to *bz*. The failure to detect *Mx* activity makes it highly unlikely that any of the *Mx*-hybridizing sequences in the tested inbreds possess *Mx* activity.

Mx Dosage Effect

Mottinger (1992) found that increasing the dosage of a *9S* chromosome arm carrying *bz-x3m* and two *Mx* elements resulted in an increase in the frequency of spots per kernel and in the frequency of kernels with larger spots, which are indicative of earlier *rMx* excision events. In that experiment, dosage of the autonomous element and the reporter allele were varied jointly. Because *Mx* is present in single copy in the W22 *Mx Sh bz-x3m* stock and absent in the derived + *sh bz-x3m* stock (Figure 3, right), it is possible to vary the dosage of *Mx*, while holding the dosage of the *bz-x3m* reporter allele constant, by crossing the two stocks reciprocally. In this reciprocal cross, kernels borne on the *Mx Sh bz-x3m* parent will have two doses of *Mx*, whereas those borne on the + *sh bz-x3m* parent will have a single dose of *Mx*. All will have three doses of the *bz-x3m* reporter. The number of spots in 75 kernels from each cross was counted and the average number of spots per kernel calculated. The averages were 3.7 in one-*Mx* kernels and 4.2 in two-*Mx* kernels. The distributions of kernel spot number in the two crosses were broad (standard deviations approaching means) and virtually identical. The spot size was small and remarkably uniform in all kernels. Thus, increasing the dosage of the *Mx* element located 2 cM distal to *c1* in *9S* from one to two does not appear to have an obvious effect on the excision of *rMx* from *bz-X3m* in a W22 background.

Transposons of the *Mx* and *Ac* Systems Do Not Cross-React

The availability of *bz* reporter alleles for *Mx* and *Ac* makes it readily feasible to test whether these two *hAT* transposon systems can cross-react with each other. To determine whether *Mx* could *trans*-activate excision of *Ds* elements from *bz*, a *bz-m2*(*D1*) stock, carrying a *Ds* deletion derivative of *Ac* in the second exon (Dooner et al., 1986), and a *Bz-wm* stock, carrying a *Ds1* element in the promoter (Schiefelbein et al., 1988), were pollinated with *Mx bz-R* as test and with *bz-R wx-m7*(*Ac*) as positive control. To determine, reciprocally, whether *Ac* could *trans*-activate excision of *rMx* from *bz-x3m*, the + *sh bz-x3m* stock was pollinated with *bz-R wx-m7*(*Ac*) as test and with *Mx bz-R* as positive control. None of the kernels from any of the test crosses were spotted, whereas most of the kernels from the

(B) Amino acid sequence alignment of the putative transposases encoded by *Mx*, *Ac*, and *Tam3*. The latter two are the main representatives of autonomous *hAT* elements from monocots and dicots, respectively. The sequences were aligned with MultiAlin, and the aligned sequences were decorated with BoxShade 3.21. Identity and similarity of amino acid residues are indicated by black and gray shading, respectively.

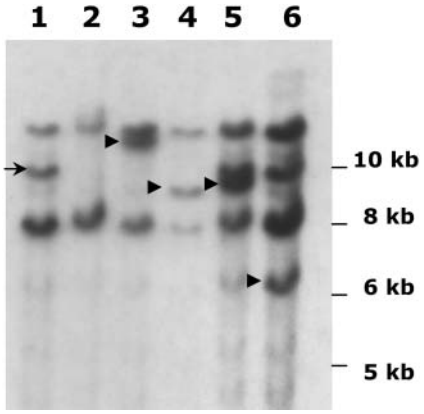

Figure 8. DNA Gel Blot Analysis of *Mx* Transposition.

Genomic DNA was digested with *Nco*I, blotted onto Nylon membranes, and hybridized to an internal *Mx* probe extending from position 761 to 1710 in the nucleotide sequence. Lane 1, *bz-x3m* stock (*Mx Sh bz-x3m*); lane 2, *Mx* tester line (+ *sh bz-x3m*); lanes 3 to 6, derivatives of the *bz-x3m* stock with transposed *Mx* elements. Arrow, original *Mx* element; arrowheads, transposed *Mx* elements.

control crosses were, indicating that *Mx* could not substitute for *Ac* nor *Ac* for *Mx*. Furthermore, ears from reciprocal crosses between *bz-m2*(*Ac*) and *bz-R* displayed the characteristic inverse dosage effect of *Ac*, independent of the *Mx* constitution of the *bz-R* stock, indicating that *Mx* did not interfere with *Ac*'s dosage effect. Thus, *Ac-Ds* and *Mx-rMx* are two active *hAT* transposon systems in the same species that have evolved different specificities and do not interact with each other.

DISCUSSION

Somatic instability of the *bz-x3m* mutation, expressed as a spotted kernel phenotype, was ascribed by Mottinger (1992) to a two-element system consisting of *rMx*, a nonautonomous transposon at *bz*, and *Mx*, an autonomous transposon located nearby. Mottinger (1973) had earlier established by conventional genetic tests that the factor responsible for the instability of *bz-x3m* did not correspond to the autonomous element of any of the major families then known. A W22 version of *bz-x3m*, developed by repeated backcrosses of the original mutant to that inbred and selection for spotted kernels, was used in this work to isolate *rMx* and *Mx*. This stock carries a single active *Mx* element at a position 6 cM distal to *sh1* on *9S*. Recombinant stocks carrying only *bz-x3m* or *Mx* were derived and used as *Mx* tester and source, respectively, in subsequent genetic tests of transposon interactions and to authenticate *Mx* candidates isolated molecularly.

The nonautonomous *rMx* element is 571 bp long, ends in 13-bp TIRs with a single internal mismatch, and is flanked by an 8-bp TSD. *rMx* retains no vestiges of a transposase (TPase)-coding sequence, but its terminal sequences resemble those of *Tz86*, a maize transposon whose ends only are known. The 181 nucleotides at the 5′ ends of *rMx* and *Tz86* are 77% identical, and the 170 nucleotides at the respective 3′ ends are 81% identical. *Tz86* has been described as a 3.6-kb transposon that generates a 10-bp TSD and lacks a discernible TIR (Dellaporta et al., 1984). A reexamination of the *Tz86-sh1* junction sequences in light of the alignment between the *Tz86* and *rMx* ends (Figure 2) leads to the revised conclusion that, like *rMx*, *Tz86* has a 13-bp imperfect TIR (TCACAGTGGGCAT at the 5′ end, and ATGCCCAGCGTGA at the 3′ end, noncomplementary bases underlined) and produces an 8-bp, rather than a 10-bp, TSD (GGCTGATG). The 13-bp TIRs of *Tz86* and *rMx* differ from each other by 3 and 4 bp, respectively, at the 5′ and 3′ ends. The internal part of *rMx* shows little similarity to the rest of the available *Tz86* sequence.

There are ~15 copies of *rMx* homologous sequences in the W22 inbred. Like most other transposons, *rMx* can excise germinally, leaving either no footprints or typical transposon footprints upon excision, and can create adjacent deletions of host DNA, probably from abortive transposition events. The germinal excision frequency of *rMx* in W22 is estimated to be at least 0.5%, based on the reversion of *bz-x3m* to *Bz′*. However, this is clearly an underestimate because *rMx* sits in the second exon of the *bz* gene and many excisions will likely produce a stable bronze phenotype. Such stable *bz* derivatives are difficult to identify because of the incomplete penetrance of the *bz-x3m* mutation. In *bz-m2*(*Ac*), a completely penetrant mutable allele that harbors an *Ac* element in the second exon of *bz*, stable *bz* derivatives outnumber *Bz′* revertants by a factor of 4 to 1 (McClintock, 1956a; Dooner and Belachew, 1989).

Because an *rMx* probe failed to reveal any bands that cosegregated with *Mx*, an iterative PCR approach was developed to isolate *Mx*. This approach, termed primer walking and diagrammed in Figure 4, is based upon the fact that all known autonomous maize transposons have defective relatives in the genome that have suffered internal deletions of variable sizes. The approach consists of amplifying internal sequences from progressively larger members of a family with primers based on

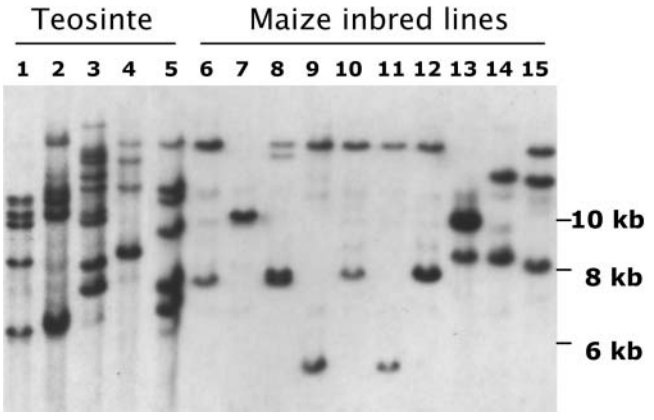

Figure 9. DNA Gel Blot Analysis of *Mx* Abundance in Maize Inbreds and Wild Relatives.

Genomic DNA was digested with *Nco*I, blotted onto Nylon membranes, and hybridized to the same internal *Mx* probe as in Figure 8. Lanes 1 and 2, *Z. mays* ssp *mexicana*, collected in Estado, Mexico; lanes 3 and 4, *Z. mays* ssp *parviglumis*, collected in Michoacán; lane 5, *Z. mays* ssp *mexicana*, collected in Michocán; lane 6, A188; lane 7, A636; lane 8, B73; lane 9, BSSS53; lane 10, 4Co63; lane 11, H99; lane 12, M14; lane 13, Mo17; lane 14, W22; lane 15, W23.

unique sequences from the last element isolated (i.e., sequences that are not shared with the smaller elements isolated earlier). A 3.7-kb element was eventually isolated and confirmed to be *Mx* on the basis of the following cosegregation and excision evidence. First, it was present in the parental *Mx bz-x3m* and recombinant *Mx bz-R* stocks, but not in the parental + *bz-R* or recombinant + *bz-x3m* stocks. Second, and more importantly, it was lost in *Mx*$^{-}$ derivatives from *Mx bz-x3m* homozygotes, where it was replaced by characteristic excision footprints at the prior site of insertion.

Mx displays features typical of other class II transposons in maize. Sequences homologous to the ends of *Mx* are present in multiple copies in the maize genome, whereas sequences homologous to the central part of *Mx* are present in low copy number (one to four) in Corn Belt inbred lines and in somewhat higher copy number in different teosinte accessions. However, none of the inbreds tested possessed *Mx* activity. Sequence analysis of *Mx* revealed it to be a member of the *hAT* superfamily of transposons, which also includes *Ac*. The transposons in this group are categorized primarily on the basis of sequence similarities between their TIRs, amino acid homology among the element-encoded TPases, and the formation of 8-bp TSDs (Kunze and Weil, 2002). Like *Ac*, *Mx* contains several copies of a hexanucleotide motif in its subterminal regions, although the hexanucleotide sequences differ. The *Mx* hexanucleotide repeat is also present in *rMx*, although in fewer copies (15 versus 17). The *Ac* TIRs and subterminal repeats have been shown to bind the *Ac* TPase in vitro (Kunze and Starlinger, 1989; Becker and Kunze, 1997) and most likely play a role in determining the specificity of transposon interactions.

Mx also resembles *Ac* in its transposition properties: transposed copies of the element can be recovered either with or without a copy of the element at the donor site. The frequency of germinal excision and loss of *Mx* from its location 6 cM distal to *sh1* in *9S* is in the low percentage (3/144), similar to that of *Ac* from *bz-m2*(*Ac*) (Dooner and Belachew, 1989). *Ac* transposes preferentially to linked sites (Greenblatt, 1984; Dooner and Belachew, 1989) and *Mx* probably does, too, based on the fact that stocks carrying *Mx* elements at three different linked locations in *9S* have been derived from the original *bz-x3m* mutant stock (Mottinger, 1992; this article). However, *Mx* may lack *Ac*'s typical negative dosage effect. *Ac* normally displays a negative dosage effect in which increasing copies of the element result in a developmental delay and reduced frequency of transpositions of either *Ac* or *Ds* (McClintock, 1952; Dellaporta and Moreno, 1994), although a few cases of *Ac* elements with either positive or no dosage effect have been described (Heinlein and Starlinger, 1991; Brutnell et al., 1997). In the original *bz-X3m* line, which had two *Mx* elements in *9S*, Mottinger (1992) reported a positive dosage effect of *Mx* on *rMx* excision, whereas in our W22 derived line, which has a single *Mx* element at a different location, we do not see an obvious effect when *Mx* dosage is increased from one to two. The absence of negative dosage effect of *Mx* on the somatic excision of *rMx* may mean that the *Mx* TPase protein does not form inactive aggregates as readily as the *Ac* TPase (Heinlein et al., 1994).

The combination of three copies of *bz-x3m* and either one or two copies of *Mx*, results in a very fine spotting pattern, indicative of infrequent and late somatic excisions (Figure 1). Interestingly, the 13-bp 5′ and 3′ TIRs of *Mx* and *rMx* are only 73% identical (19/26). This is the highest degree of divergence found between the TIRs of an autonomous and a nonautonomous member of a transposon family in plants and suggests that *Mx* and *rMx* could be elements that are diverging from each other, yet can still interact so that the genetic complementation test places them in the same family. Analysis of the extensive collection of maize sequences in the Genome Survey Sequence section of GenBank supports this view. Searches of that database using as queries the 5′ and 3′ terminal 180 nucleotides of *Mx* and *rMx*, which contain the elements' TIRs and all the subterminal hexanucleotide repeats, yielded sequences that shared TIRs with *rMx* and were more similar to the ends of *rMx* than of *Mx* (81 to 96% versus 57 to 72% identity at the 5′ end and 85 to 96% versus 63 to 72% identity at the 3′ end; see Supplemental Table 1 online) and sequences that, conversely, shared TIRs with *Mx* and were more similar to the ends of *Mx* than of *rMx* (82 to 99% versus 63 to 71% identity at the 5′ end and 89 to 98% versus 64 to 75% identity at the 3′ end; see Supplemental Table 1 online). This indicates that maize has several defective transposons, such as *dMx1*, that are more closely related to *Mx* than *rMx*, its genetically defined nonautonomous partner, and whose terminal sequences may be better substrates for the *Mx* TPase than those of *rMx*. In *Ac*, both the TIRs and the subterminal repeats bind to the TPase and are required for *Ac* excision (Feldmar and Kunze, 1991; Becker and Kunze, 1996; Weil and Kunze, 2000). By analogy, both the TIRs and the hexanucleotide repeats at either end are probably involved in the transposition of *Mx* and *rMx*. Perhaps the rather low somatic and germinal excision of *rMx* from *bz-x3m* is because of an inefficient interaction between the *Mx* TPase and the *rMx* TIRs. If so, a reporter allele harboring a defective transposon of the *dMx1* type might be expected to produce a more highly mutable phenotype than *bz-x3m* in the presence of *Mx*.

The evolution of the *hAT* transposon superfamily has been studied by many investigators (Kempken and Windhofer, 2001; Rubin et al., 2001; Robertson, 2002). These studies have revealed that the *hAT* superfamily is very ancient, probably predating the plant–fungi–animal split 1000 million years ago. To examine the relationship of *Mx* to other *hAT* transposons, a similar analysis was performed with 31 hAT TPases from plants, animals, and fungi (see Methods for the basis of selecting sequences). The amino acid sequences were aligned by ClustalX, and the phylogenetic tree shown in Figure 10 was constructed using neighbor joining in MEGA version 2.1 (Kumar et al., 2001). The phylogenetic analysis allows the following main conclusions.

First, and as noted by others (Kempken and Windhofer, 2001; Robertson, 2002), the plant *hAT* transposons fall into different clades. One clade contains the genetically defined elements *Ac* (Pohlman et al., 1984); (Muller-Neumann et al., 1984), *Tam3* (Hehl et al., 1991), and *Slide* (Grappin et al., 1996) from maize, Antirrhinum, and tobacco (*Nicotiana tabacum*), respectively, plus several Arabidopsis and rice homologs. Another clade includes *Tip100* from morning glory (*Ipomoea tricolor*; Ishikawa et al., 2002), *I-R* from maize (W. Eggleston, personal communication), and a transposon from the mosquito *Anopheles gambia*. The more distantly related elements *Bg* from maize (Hartings et al., 1991a) and *Tag1* from Arabidopsis (Liu and Crawford,

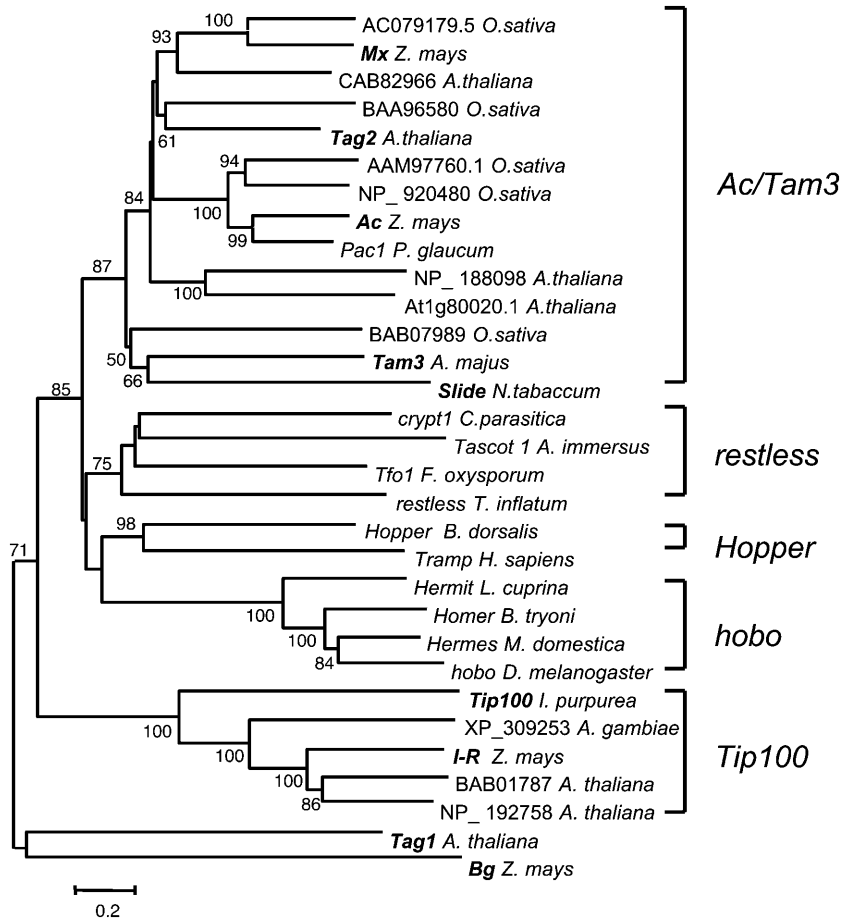

Figure 10. Phylogenetic Tree of *hAT* Transposases.

Sequences were aligned using ClustalX, and the tree was constructed using neighbor joining in MEGA version 2.1. Each sequence is identified by either its transposon name or GenBank accession number and the name of its source species. Plant autonomous elements are indicated in bold. Numbers above the branches indicate the percentage of 1000 bootstrap replications in which that branch was present. The well-supported clades are indicated by brackets and given the name of the first described element(s) in that clade.

1998) do not belong to either of the above clades and may form yet a third, albeit weakly supported, group. Hence, it is not surprising that *Ac* and *Bg* do not cross-mobilize each other's defective elements (Hartings et al., 1991b).

Second, the *Mx* element falls in the same clade as *Ac* and is closely related to it. Yet, although *Ac* and *Mx* are much closer to each other, they still do not interact: *Mx* cannot *trans*-activate *Ds* excision nor contribute to *Ac*'s dosage effect. Thus, modern maize has several families of active and noninteracting transposable elements belonging to the same *hAT* superfamily. If one adds to the above three, *Dt* (Rhoades, 1938) and *I-R* (Eggleston et al., 1995), which have been demonstrated not to interact genetically with *Ac* and whose partial molecular characterization classifies them as *hAT* elements (Kunze and Weil, 2002; Robertson, 2002), then there may be at least five families of noninteracting *hAT* elements of different degree of relatedness in a single species. This observation raises the interesting question of how transposons of the same superfamily can evolve different specificities within one species.

Transposons of the *Tc1/mariner* superfamily appear to have spread frequently by horizontal transfer during evolution (Hartl et al., 1997; Robertson, 2002). Lampe et al. (2001) have explained the coexistence of distinct autonomous *mariner* elements in the same genome by a model that invokes transposon amplification, inactivation of most copies by a variety of mechanisms leading to stabilization of the transposon copy number, accumulation of neutral or functionally different mutations in active copies, and horizontal transfer of a divergent functional copy to another species. After horizontal transfer, any mutation that increased the element's activity would be of benefit to the element, as long as it did not affect the fitness of the host. One such mutation would be a *cis*-acting suppressor mutation in the TIR. If this process was repeated several times, new elements would be expected to diverge from the original to the point that they would no longer interact if they came together again in the same organism. In this model, mutations in the TPase and the TIRs that lead to novel transposon specificities occur in separate organisms.

Unlike the situation with *Tc1/mariner* elements, there is currently no compelling evidence that transposons of the *hAT* superfamily have undergone horizontal transfer in evolution. In fact, Rubin et al. (2001) concluded that, in contrast with what had been proposed earlier (Calvi et al., 1991), there was no evidence for transkingdom horizontal transfer of *hAT* elements and that the question of intrakingdom horizontal transfer could not be resolved from the available data. Therefore, a different model for the evolution of transposon specificities may need to be invoked to explain the cooccurrence of different *hAT* autonomous elements in the same species.

The following model assumes that hAT TPases resemble the *Ac* TPase in possessing a dimerization domain (hAT3), which is essential for enzyme activity and also plays a role in the formation of inactive aggregates, although an additional, as yet uncharacterized, domain is also required for *Ac* multimer formation (Essers et al., 2000; Kunze and Weil, 2002). A mutation in the TPase dimerization domain would allow the new TPase to escape inactivation if the new monomer failed to heterodimerize with the original, more abundant TPase monomers (or did so poorly), but was still able to form active homodimers. Consequently, the new TPase would contribute disproportionately to total activity because it would escape the aggregation inactivation mechanism of the original TPase. However, this will not affect the relative numbers of old and new transposons until the latter's TIRs change, likely in two steps, to favor their recognition by the new TPase. First, a chance mutation in the TIR of one of the more numerous original elements, followed by the homogenization of both TIRs by a conversion-like mechanism, would produce an element that would serve as a better substrate for the new TPase. Thereafter, the relative copy number of that element will increase in individuals that also harbor the element encoding the new TPase. This differential amplification will enhance the probability that the original TPase gene carried in one of the elements with modified TIRs will be replaced with a new TPase gene by mechanisms such as ectopic gene conversion or template switching during the occasional gap repair that follows *hAT* element excision (Yan et al., 1999). The resulting new element and its progenitor will begin to evolve independently of each other because their oligomerization inactivation mechanisms would not cross-react. *Mx* and *rMx*, with their unusually divergent TIRs, may represent transposons in the process of evolving different specificities. If so, an autonomous element with *rMx*-like ends and encoding a TPase closely related to, but different from, that of *Mx* may be present in maize.

METHODS

Plant Materials

The *bz-x3m* mutation was obtained from John Mottinger, backcrossed four times to a W22 stock carrying the *bz-R* allele, and selfed twice to derive the *bz-x3m* stock used in this work. All other stocks were also in a W22 background. *bz-R* is the stable reference allele for the *bz* locus. The mutable alleles *bz-m2*(*D1*), *Bz-wm*, and *wx-m7*(*Ac*) were obtained from B. McClintock (McClintock, 1962, 1964). A188, A636, B73, BSSS53, 4Co63, H99, M14, Mo17, and W23 are standard maize (*Zea mays*) inbred lines from various public breeding programs (Gerdes et al., 1993). The teosinte accessions were from collections made by Jerry Kermicle in various Mexican states.

PCR and Sequencing

PCR was performed according to the protocol of QiaTaq (Qiagen, Valencia, CA). The fragment containing *rMx* was amplified from genomic DNA of the *bz-x3m* mutant using the pair of *bz* primers Bz-C (5′-CTCAACACGTTCCCAGGC-3′) and Bz-3R (5′-AAACCTCTGAACAGCAAGACGACC-3′). These primers are located 591 bp upstream and 172 bp downstream, respectively, of the *rMx* insertion site. Germinal *rMx* excision sites were amplified using the genomic DNAs of *Bz′/bz-R* revertants as templates and primers Bz-C and Bz-3R. The sequence corresponding to primer Bz-C is deleted from the *bz-R* allele (Ralston et al., 1988), so only the *bz* fragment from the *Bz′* revertant allele is amplified in the reaction. The sequences of the six oligonucleotide primers used for the primer walking method diagrammed in Figure 4 are as follows: p1, 5′-CACTGGGCATAAAACCCGAGCCC-3′; p2, 5′-CTGGGCATTCGGGTTAGCCCGAA-3′; p3, 5′-CGGGCTTAATCGGGTAGCAACACC-3′; p4, 5′-CCGTTCTACCCGATTTCGTTGCAG-3′; p5, 5′-GTACACCTGGCCGGATCCGTTCAA-3′; p6, 5′-CCAGTAGACTTGCTGCTCACTGGT-3′.

The *Mx* flanking fragment (*tmx*) was isolated by IPCR, as optimized in our lab (Cowperthwaite et al., 2002), using genomic DNA from the *bz-x3m* mutant as template. The primers used in the IPCR are as follows: dMx2-5′R, 5′- AAGCCGGATGCTCCAGACGGCCAC-3′, and dMx2-3′F, 5′- GTGTTGTACGCTTCTGCTAGTGTA-3′. The *Mx* element was amplified from the W22 *bz-x3m* stock using primers based on *tmx*. These primers are tMx-5′-1F (5′-TCGACGTCCGTGATCAACGCCGTT-3′) and tMx-3′-2R (5′-GGCGAAAAAGAACAGTGGGCGCAC-3′). The *Mx* germinal excision sites (empty sites) were amplified from the *tmx′ Sh bz-x3m/+ sh bz-R* heterozygotes using primers tMx-5′-1F and tMx-3′-2R. These PCR products were then run on 8% PAGE gels to detect size differences between the amplified alleles. The PCR products were cloned into pGEM-T easy (Promega, Madison, WI) and transformed into DH5α competent cells. Plasmids were purified with a Qiagen spin miniprep kit. Eight randomly selected clones from each empty site amplification were sequenced to characterize the footprints of *Mx* excision. DNA sequencing was performed in an ABI 377 sequencer (Perkin-Elmer, Torrance, CA) following the manufacturer's instructions. The sequences of *Mx* and *rMx* have been submitted to and are being processed by GenBank.

Nucleic Acid Extraction and Hybridization

Genomic DNA from seedlings and mature leaves was prepared by a urea extraction procedure (Greene et al., 1994). A total of 15 to 20 μg of genomic DNA was digested with various restriction enzymes (New England Biolabs, Beverly, MA), resolved on a 0.8% agarose gel in Tris acetate EDTA buffer, and transferred a to Hybond N^+ membrane according to the manufacturer's protocol (Amersham Biosciences, Buckinghamshire, UK). Radioactive probes were prepared with a Ready-to-Go labeling kit (Amersham Biosciences). Membrane hybridization and washing conditions followed the recommendations of the manufacturer. The fragment for the *dMx2* probe was released from the dMx2-pGEM-T easy clone by *Eco*RI digestion. The primers used for generating the *Mx* internal probe, with their *Mx* location indicated in parentheses, are Mx-5′-2F (760 to 783) and Mx-3′-4R (1686 to 1710). The fragment for the *tmx* probe ($\sim$280 bp long) was amplified from genomic DNA of the W22 *bz-R* stock, using primers tMx-5′-1F and tMx-3′-1R (5′-GCGCTAAACTAATGCGGAAAGAGG-3′), cloned into pGEM-T easy, and sequenced.

Chromosome Mapping

Recombinant inbred (RI) lines from a cross between T232 and CM37 were used in chromosome mapping (Burr et al., 1988). Gels were blotted onto

Hybond N^+ membranes and hybridized with a radiolabeled *Mx*-adjacent fragment (*tmx*). Several restriction enzymes were tested on the parental genomic DNA, and *Eco*RI gave the most distinct restriction fragment length polymorphisms. The segregation of restriction fragment length polymorphisms in RI populations was scored and compared with the RI database at Brookhaven National Lab.

Phylogenetic Analysis

Initial BlastX searches of the GenBank nonredundant databases were performed using the *Mx* sequence as query and limiting the searches to viridiplantae, fungi, and metazoa, respectively. Hits containing an open reading frame longer than 400 amino acids were chosen for further analysis. Some *hAT* transposons of the more distant *Tip100* group (Robertson, 2002), which were not recovered initially, were also incorporated in the phylogenetic analysis. The putative *Slide* transposase sequence was deduced from the homology of its predicted open reading frames to other hAT transposases in the database. To reduce the redundancy within the data, sequences with a high degree of similarity to another sequence from the same species were eliminated so that only one of them was included in the comparison. The full-length amino acid sequences were aligned by ClustalX (Thompson et al., 1997), and a phylogenetic tree was constructed using neighbor joining in MEGA version 2.1 (http://www.megasoftware.net/), with 1000 bootstrap replicates and the pairwise-deletion option for handling gaps.

Sequence data for *Mx*, *rMx*, *dMx1*, and *dMx2* have been deposited with the EMBL/GenBank data libraries under accession numbers AY753670, AY753671, AY786440, and AY786441, respectively.

ACKNOWLEDGMENTS

We thank members of the Dooner lab, particularly Yubin Li, for comments on the manuscript, John Mottinger for seeds of the *bz-x3m* mutation, Bill Eggleston for the unpublished sequence of *I-R*, Brandon Gaut and Chunguang Du for help with the phylogenetic analysis, and Ben Burr for the analysis of the RI mapping data. This research was supported by a Busch-Waksman Predoctoral Fellowship from Rutgers University to Z.X. and National Science Foundation Grant MCB 99-04646 and Waksman Institute start-up funds to H.K.D.

Received September 17, 2004; accepted November 16, 2004.

REFERENCES

Arabidopsis Genome Initiative (2000). Analysis of the genome sequence of the flowering plant *Arabidopsis thaliana*. Nature **408,** 796–815.

Becker, H.A., and Kunze, R. (1996). Binding sites for maize nuclear proteins in the subterminal regions of the transposable element *Activator*. Mol. Gen. Genet. **251,** 428–435.

Becker, H.A., and Kunze, R. (1997). Maize *Activator* transposase has a bipartite DNA binding domain that recognizes subterminal sequences and the terminal inverted repeats. Mol. Gen. Genet. **254,** 219–230.

Brink, R.A. (1956). A genetic change associated with the *R* locus in maize which is directed and potentially reversible. Genetics **41,** 872–889.

Brink, R.A., and Nilan, R.A. (1952). The relation between light variegated and medium variegated pericarp in maize. Genetics **37,** 519–544.

Brown, J.J., Mattes, M.G., O'Reilly, C., and Shepherd, N.S. (1989). Molecular characterization of *rDt*, a maize transposon of the *Dotted* controlling element system. Mol. Gen. Genet. **215,** 239–244.

Brutnell, T.P., May, B.P., and Dellaporta, S.L. (1997). The Ac-st2 element of maize exhibits a positive dosage effect and epigenetic regulation. Genetics **147,** 823–834.

Burr, B., Burr, F.A., Thompson, K.H., Albertson, M.C., and Stuber, C.W. (1988). Gene mapping with recombinant inbreds in maize. Genetics **118,** 519–526.

Calvi, B.R., Hong, T.J., Findley, S.D., and Gelbart, W.M. (1991). Evidence for a common evolutionary origin of inverted repeat transposons in Drosophila and plants: *hobo*, *Activator*, and *Tam3*. Cell **66,** 465–471.

Chen, J., Greenblatt, I.M., and Dellaporta, S.L. (1987). Transposition of *Ac* from the *P* locus of maize into unreplicated chromosomal sites. Genetics **117,** 109–116.

Chen, J., Greenblatt, I.M., and Dellaporta, S.L. (1992). Molecular analysis of *Ac* transposition and DNA replication. Genetics **130,** 665–676.

Cone, K.C., et al. (2002). Genetic, physical, and informatics resources for maize. On the road to an integrated map. Plant Physiol. **130,** 1598–1605.

Cormack, J.B., Cox, D.F., and Peterson, P.A. (1988). Presence of the transposable element *Uq* in maize breeding material. Crop Sci. **28,** 941–944.

Cowperthwaite, M., Park, W., Xu, Z., Yan, X., Maurais, S.C., and Dooner, H.K. (2002). Use of the transposon Ac as a gene-searching engine in the maize genome. Plant Cell **14,** 713–726.

Dellaporta, S.L., Chomet, P.S., Mottinger, J.P., Wood, J.A., Yu, S.M., and Hicks, J.B. (1984). Endogenous transposable elements associated with virus infection in maize. Cold Spring Harb. Symp. Quant. Biol. **49,** 321–328.

Dellaporta, S.L., and Moreno, M.A. (1994). Gene tagging with *Ac*/*Ds* elements in maize. In The Maize Handbook, M. Freeling and V. Walbot, eds (New York: Springer Verlag), pp. 219–233.

Dennis, E.S., Finnegan, E.J., Taylor, B.H., Peterson, T.A., Walker, A.R., and Peacock, W.J. (1988). Maize transposable elements: Structure, function, and regulation. In Plant Transposable Elements, O.E. Nelson, ed (New York: Plenum Press), pp. 101–113.

Dooner, H.K. (1985). A deletion adjacent to the *Ac* insertion site in a stable *bz* derivative from *bz-m2*(*Ac*). In Plant Genetics, M. Freeling, ed (New York: Alan R. Liss), pp. 561–573.

Dooner, H.K., and Belachew, A. (1989). Transposition pattern of the maize element *Ac* from the *bz-m2*(*Ac*) allele. Genetics **122,** 447–457.

Dooner, H.K., English, J., Ralston, E., and Weck, E. (1986). A single genetic unit specifies two transposition functions in the maize element *Activator*. Science **234,** 210–211.

Eggleston, W.B., Alleman, M., and Kermicle, J.L. (1995). Molecular organization and germinal instability of *R-stippled* maize. Genetics **141,** 347–360.

Essers, L., Adolphs, R.H., and Kunze, R. (2000). A highly conserved domain of the maize *Activator* transposase is involved in dimerization. Plant Cell **12,** 211–224.

Fedoroff, N. (1983). Controlling elements in maize. In Mobile Genetic Elements, J.A. Shapiro, ed (New York: Academic Press), pp. 1–63.

Feldmar, S., and Kunze, R. (1991). The ORFa protein, the putative transposase of maize transposable element Ac, has a basic DNA binding domain. EMBO J. **10,** 4003–4010.

Feschotte, C., Jiang, N., and Wessler, S.R. (2002a). Plant transposable elements: Where genetics meets genomics. Nat. Rev. Genet. **3,** 329–341.

Feschotte, C., Zhang, Y., and Wessler, S.R. (2002b). Miniature inverted repeat transposable elements and their relationship to

established DNA transposons. In Moble DNA II, N.L. Craig, R. Craigie, M. Gellert, and A.M. Lambowitz, eds (Washington, D.C.: ASM Press), pp. 1147–1158.

Gerdes, J.T., Behr, C.F., Coors, J.G., and Tracy, W.F. (1993). Compilation of North American Maize Breeding Germplasm. (Madison, WI: Crop Science Society of America).

Goff, S.A., et al. (2002). A draft sequence of the rice genome (*Oryza sativa* L. ssp. *japonica*). Science **296,** 92–100.

Gonella, J.A., and Peterson, P.A. (1977). Controlling elements in a tribal maize from Colombia: *Fcu*, a two-unit system. Genetics **85,** 629–645.

Grappin, P., Audeon, C., Chupeau, M.C., and Grandbastien, M.A. (1996). Molecular and functional characterization of Slide, an Ac-like autonomous transposable element from tobacco. Mol. Gen. Genet. **252,** 386–397.

Greenblatt, I.M. (1984). A chromosome replication pattern deduced from pericarp phenotypes resulting from movement of the transposable element *Modulator* in maize. Genetics **108,** 471–485.

Greenblatt, I.M., and Brink, R.A. (1962). Twin mutations in medium variegated pericarp maize. Genetics **47,** 489–501.

Greene, B., Walko, R., and Hake, S. (1994). Mutator insertions in an intron of the maize *knotted1* gene result in dominant suppressible mutations. Genetics **138,** 1275–1285.

Hartings, H., Rossi, V., Lazzaroni, N., Thompson, R.D., Salamini, F., and Motto, M. (1991a). Nucleotide sequence of the *Bg* transposable element of *Zea mays* L. Maydica **36,** 355–359.

Hartings, H., Spilmont, C., Lazzaroni, N., Rossi, V., Salamini, F., Thompson, R.D., and Motto, M. (1991b). Molecular analysis of the *Bg-rbg* transposable element system of *Zea mays* L. Mol. Gen. Genet. **227,** 91–96.

Hartl, D.L., Lohe, A.R., and Lozovskaya, E.R. (1997). Modern thoughts on an ancyent marinere: Function, evolution, regulation. Annu. Rev. Genet. **31,** 337–358.

Hehl, R., Nacken, W.K., Krause, A., Saedler, H., and Sommer, H. (1991). Structural analysis of *Tam3*, a transposable element from *Antirrhinum majus*, reveals homologies to the *Ac* element from maize. Plant Mol. Biol. **16,** 369–371.

Heinlein, M., Brattig, T., and Kunze, R. (1994). In vivo aggregation of maize Activator (Ac) transposase in nuclei of maize endosperm and Petunia protoplasts. Plant J. **5,** 705–714.

Heinlein, M., and Starlinger, P. (1991). Variegation patterns caused by transposable element *Ac*. Maydica **36,** 309–316.

Ishikawa, N., Johzuka-Hisatomi, Y., Sugita, K., Ebinuma, H., and Iida, S. (2002). The transposon *Tip100* from the common morning glory is an autonomous element that can transpose in tobacco plants. Mol. Genet. Genomics **266,** 732–739.

Kempken, F., and Windhofer, F. (2001). The *hAT* family: A versatile transposon group common to plants, fungi, animals, and man. Chromosoma **110,** 1–9.

Kumar, S., Tamura, K., Jakobsen, I.B., and Nei, M. (2001). Molecular Evolutionary Genetics Analysis (MEGA) Software. (Tempe, AZ: Arizona State University).

Kunze, R., and Starlinger, P. (1989). The putative transposase of transposable element *Ac* from *Zea mays* L. interacts with subterminal sequences of *Ac*. EMBO J. **8,** 3177–3185.

Kunze, R., and Weil, C.F. (2002). The *hAT* and CACTA superfamilies of plant transposons. In Mobile DNA II, N.L. Craig, R. Craigie, M. Gellert, and A.M. Lambowitz, eds (Washington, D.C.: ASM Press), pp. 565–610.

Lampe, D.J., Walden, K.K., and Robertson, H.M. (2001). Loss of transposase-DNA interaction may underlie the divergence of *mariner* family transposable elements and the ability of more than one mariner to occupy the same genome. Mol. Biol. Evol. **18,** 954–961.

Liu, D., and Crawford, N.M. (1998). Characterization of the putative transposase mRNA of *Tag1*, which is ubiquitously expressed in Arabidopsis and can be induced by Agrobacterium-mediated transformation with *dTag1* DNA. Genetics **149,** 693–701.

McClintock, B. (1952). Chromosome organization and gene expression. Cold Spring Harb. Symp. Quant. Biol. **16,** 13–47.

McClintock, B. (1956a). Mutation in maize. Carnegie Inst. Wash. Yrbk. **55,** 323–332.

McClintock, B. (1956b). Intranuclear systems controlling gene action and mutation. Brookhaven Symp. Biol. **8,** 58–74.

McClintock, B. (1962). Topographical relations between elements of control systems in maize. Carnegie Inst. Wash. Yrbk. **61,** 448–461.

McClintock, B. (1964). Aspects of gene regulation in maize. Carnegie Inst. Wash. Yrbk. **63,** 592–602.

Montanelli, C., Di Fonzo, N., Marotta, R., Soave, C., and Salamini, F. (1984). Occurrence and behavior of the components of the *o2-m(r)-Bg* system of maize controlling elements. Mol. Gen. Genet. **197,** 209–218.

Mottinger, J. (1973). Unstable mutants of *bronze* induced by premeiotic X-ray treatment in maize. Theor. Appl. Genet. **43,** 190–195.

Mottinger, J.P. (1992). Studies on the *Mx* transposable element system in maize recovered from X-irradiated stocks. Mol. Gen. Genet. **236,** 96–104.

Mottinger, J.P., Dellaporta, S.L., and Keller, P.B. (1984). Stable and unstable mutations in Aberrant Ratio stocks of maize. Genetics **106,** 751–767.

Muller-Neumann, M., Yoder, J., and Starlinger, P. (1984). The DNA sequence of the transposable element *Ac* of *Zea mays* L. Mol. Gen. Genet. **198,** 19–24.

Neuffer, M.G., Coe, E.H., and Wessler, S. (1997). The Mutants of Maize. (Cold Spring Harbor, NY: Cold Spring Harbor Laboratory Press).

Palaisa, K.A., Morgante, M., Williams, M., and Rafalski, A. (2003). Contrasting effects of selection on sequence diversity and linkage disequilibrium at two phytoene synthase loci. Plant Cell **15,** 1795–1806.

Panavas, T., Weir, J., and Walker, E.L. (1999). The structure and paramutagenicity of the *R-marbled* haplotype of *Zea mays*. Genetics **153,** 979–991.

Peterson, P.A. (1988). The mobile element systems in maize. In Plant Transposable Elements, O.E. Nelson, ed (New York: Plenum Press), pp. 43–68.

Peterson, P.A., and Salamini, F. (1986). A search for active mobile elements in the Iowa Stiff Stalk Synthetic maize population and some derivatives. Maydica **31,** 163–172.

Pohlman, R., Fedoroff, N., and Messing, J. (1984). The nucleotide sequence of the maize controlling element *Activator*. Cell **37,** 635–644.

Ralston, E.J., English, J., and Dooner, H.K. (1988). Sequence of three *bronze* alleles of maize and correlation with the genetic fine structure. Genetics **119,** 185–197.

Rhoades, M.M. (1938). Effect of the *Dt* gene on the mutability of the *a1* allele in maize. Genetics **23,** 377–397.

Rhoades, M.M., and Dempsey, E. (1982). The induction of mutable systems in plants with the high-loss mechanism. Maize Genet. Coop. News Lett. **56,** 21–26.

Robertson, H.M. (2002). Evolution of DNA transposons in eukaryotes. In Mobile DNA II, N.L. Craig, R. Craigie, M. Gellert, and A.M. Lambowitz, eds (Washington, D.C.: ASM Press), pp. 1093–1110.

Rubin, E., Lithwick, G., and Levy, A.A. (2001). Structure and evolution of the *hAT* transposon superfamily. Genetics **158,** 949–957.

Schiefelbein, J.W., Furtek, D.B., Dooner, H.K., and Nelson, O.E., Jr. (1988). Two mutations in a maize *bronze1* allele caused by transposable elements of the *Ac-Ds* family alter the quantity and quality of the gene product. Genetics **120,** 767–777.

Shepherd, N.S., Rhoades, M.M., and Dempsey, E. (1989). Genetic and molecular characterization of *a-mrh-Mrh*, a new mutable system of *Zea mays*. Dev. Genet. **10,** 507–519.

Taylor, L.P., and Walbot, V. (1985). A deletion adjacent to the maize transposable element *Mu1* accompanies loss of *Adh1* expression. EMBO J. **4,** 869–876.

Thompson, J.D., Gibson, T.J., Plewniak, F., Jeanmougin, F., and Higgins, D.G. (1997). The CLUSTAL_X windows interface: Flexible strategies for multiple sequence alignment aided by quality analysis tools. Nucleic Acids Res. **25,** 4876–4882.

van der Walt, W.J., and Brink, R.A. (1969). Geographic distribution of paramutable and paramutagenic *R* alleles in maize. Genetics **61,** 677–695.

Walbot, V., and Rudenko, G.N. (2002). *MuDR*/*Mu* transposable elements of maize. In Mobile DNA II, N.L. Craig, R. Craigie, M. Gellert, and A.M. Lambowitz, eds (Washington, D.C.: ASM Press), pp. 533–564.

Weil, C.F., and Kunze, R. (2000). Transposition of maize *Ac*/*Ds* transposable elements in the yeast *Saccharomyces cerevisiae*. Nat. Genet. **26,** 187–190.

Xu, Z., Yan, X., Maurais, S., Fu, H., O'Brien, D.G., Mottinger, J., and Dooner, H.K. (2004). Jittery, a *Mutator* distant relative with a paradoxical mobile behavior: Excision without reinsertion. Plant Cell **16,** 1105–1114.

Yan, X., Martinez-Ferez, I.M., Kavchok, S., and Dooner, H.K. (1999). Origination of *Ds* elements from *Ac* elements in maize: Evidence for rare repair synthesis at the site of *Ac* excision. Genetics **152,** 1733–1740.